



## Postnatal renal tubule development in inbred indigenous rabbit (*Oryctolagus Cuniculus*): A histological and immunohistochemical analysis

R.S. Habib<sup>1</sup>  and A.G. Alhaaik<sup>2</sup> 

<sup>1</sup>Department of Theriogenology, Anatomy, and Physiology, College of Veterinary Medicine, University of Duhok, Duhok,

<sup>2</sup>Department of Anatomy and Histology, College of Veterinary Medicine, University of Mosul, Mosul, Iraq

### Article information

#### Article history:

Received 14 January, 2025

Accepted 01 May, 2025

Published 08 November, 2025

#### Keywords:

Histology

Immunohistochemistry

Postnatal renal development

Renal tubules

#### Correspondence:

A.G. Alhaaik

[alhaaik\\_ag@uomosul.edu.iq](mailto:alhaaik_ag@uomosul.edu.iq)

### Abstract

This study investigates postnatal renal tubules development in inbred indigenous rabbits (*Oryctolagus cuniculus*), examining histological, histochemical, morphometric, and immunohistochemical characteristics from birth to 40 days old. Fifty rabbits were categorized into five age groups based on postnatal days (PNDs) 1, 10, 15, 30, and 40. Kidneys were fixed, processed, and sectioned for hematoxylin and eosin and PAS-Alcian Blue staining, followed by microscopic examination. Immunohistochemical analysis used Anti-Lgr5 antibody to detect stem cells. Morphometric measurements were taken manually with a USB digital camera. The findings indicate that while renal tubules in one day aged rabbits had completed histogenesis through the embryonic life, they continued to develop until PND 40. A regular decrement in the epithelial height and lumen diameter of proximal and distal convoluted tubules (PCT and DCT) was observed, with PCT showing reductions of 2.3-fold and 2.1-fold, respectively, and DCT displaying a 3.5-fold decrease in lumen diameter and a 1.5-fold reduction in epithelial height. Intriguingly, Lgr5 expression, absent in PCT and DCT, was detected in interstitial tissues surrounding the LoH, with moderate expression at PND 1, gradually declining thereafter. These findings provide valuable insights into renal tubule maturation and lay a foundation for future research in renal development and regenerative medicine.

DOI: [10.33899/ijvs.2025.156567.4086](https://doi.org/10.33899/ijvs.2025.156567.4086), ©Authors, 2025, College of Veterinary Medicine, University of Mosul.

This is an open access article under the CC BY 4.0 license (<http://creativecommons.org/licenses/by/4.0/>).

### Introduction

Renal development involves morphological formation and the attainment of functional capability, starting with embryonic nephron synthesis and continuing postnatally to reach adult levels (1,2). It involves complex interactions between the ureteric bud (UB) and metanephric mesenchyme (MM), where progenitor cells support UB branching and nephron differentiation (3). In rabbits, nephrogenesis completes within 2-3 weeks postnatally, with well-developed renal loops (4). By two months, the adult nephron structure is fully established (5). While postnatal renal development has been extensively studied in murine models, research on rabbits remains limited. Notably, no studies have

immunohistochemically assessed renal stem cells using the anti-leucine-rich repeat-containing G protein-coupled receptor 5 (Lgr5) marker in renal tubules. This study is the first to provide a comprehensive analysis of postnatal renal tubule development in rabbits, integrating histological, histochemical, histo-morphometrical, and immunohistochemical (IHC) evaluations. Of importance, unlike other organs, kidneys exhibit limited regenerative capacity, except in cases of acute proximal tubule injury (6). In rabbits, the renal tubules exhibit distinct structural and functional features compared to other mammals. The proximal convoluted tubule (PCT) transitions gradually from S2 to S3, unlike the abrupt transition observed in rats and dogs (7). The brush border in the S3 segment varies across

species, being shorter in rabbits, taller in rats, and intermediate in humans (8). The loop of Henle (LoH) in rabbits is predominantly long 70%, whereas 30% are short, influencing urine concentration efficiency (9). Unlike highly urine-concentrating mammals such as rats and Psammomys, which have complex medullary vasculature, rabbits have simpler ascending and descending vasa recta (10,11). Differences in the collecting duct (CD) further highlight species variations; intercalated cells constitute 10-15% of the inner stripe of the outer medullary CD in rabbits, compared to 33% in rats, with none in the initial inner medullary CD (12). The isolation and identification of progenitor cells newly formed nephron using newly discovered markers could significantly advance our understanding of nephrogenesis, which is vital for the clinical managing of mature kidney diseases through regenerative medicine (13). Wnt signaling, particularly Wnt9b and Wnt4, is essential in regulating the activity of primary stem cells which contribute to the development of kidney (14,15). Lgr5, a direct Wnt-target gene, is documented epithelial stem/progenitor cells marker in the organs with high Wnt-dependent regeneration. While absent in adult murine kidneys, Lgr5 is strongly expressed in neonatal kidneys in mice and rabbits (13,16), localized in S-shaped bodies and cells of cortex till postnatal day (PND) 7. Lgr5 marker used in experimental animals could be crucial for understanding nephron progenitor cell roles in kidney development and isolating human nephron stem cells for therapeutic purposes.

Hence, this study aims to provide morphological and morphometric insights into development of rabbit renal tubules from PND 1 to PND 40. It evaluates the countenance levels and distribution of Lgr5 in the rabbit kidney as a marker for stem tubular cells, potentially donating to tissue repair, regeneration and renal histogenesis and offering a foundation for assessing upcoming regenerative therapies for kidney.

## **Materials and methods**

### **Ethical approval**

All animal experiments were euthanized according ethical guidelines of the scientific committee in the University of Duhok, College of Veterinary Medicine (Ref. No. CVM201910UD; 1-10-2019).

### **Sampling and study plan**

This cross-sectional study involved histological, histochemical, morphometrical, and IHC analyses. Sampling occurred from March 2021 to January 2022, using kidneys from inbred indigenous rabbits (*Oryctolagus cuniculus*) collected postnatally up to 40 days. The research was carried out at three locations: University of Duhok's animal house, Vin Medical Laboratory, and RNA Research Laboratory. A total of six adult rabbits (five females and one male) were procured, clinically assessed, and bred in a controlled

environment. After acclimatization, 50 rabbits, irrespective of sex, were allocated into five groups of ten kits each: Group 1 consisted of 1-day-old suckling kits, Group 2 included 10-day-old suckling kits, Group 3 comprised 15-day-old kits consuming both milk and solid food, Group 4 contained 30-day-old weaned kits fed on green food, and Group 5 encompassed 40-day-old post-weaned kits on a diet of solid and green food.

### **Kidney preparation**

All animals were anesthetized through intramuscular injection of ketamine at a dosage 29.1 mg / kg and xylazine at 4.3 mg/kg. Subsequently, then euthanizing by intravenous dose of 600 mg of ketamine as described by Baneux (17). Following euthanasia, the kidneys were excised, thoroughly rinsed with normal saline, and 10% neutral buffer formalin was used as fixative for 24 to 48 hours at a pH of 7.2±0.5 (18).

### **Microscopic approaches and histological processing**

Following fixation in a 10% NBF, the tissues underwent routine histological processing, histological sections of 5 micrometers were obtained using a rotary microtome. Various staining techniques, including hematoxylin and eosin (H&E) and Periodic Acid Schiff-Alcian Blue (PAS-AB), were applied to analyze tissue structure and identify polysaccharides and mucins (19). The stained slides were subsequently examined under a light microscope (Olympus), with images captured for further analysis. Additionally, following slide preparation, various micro-morphometric characteristics of renal tubules were measured by using manual measurement procedure for all study groups with the aid of USB digital Omax camera 18.0 MP (A35180U3; USA). The image processing software utilized included built-in calibration and scale bar determination, which was automated using a stage micrometer via Omax camera software. The software provided a comprehensive set of dimensional measurement tools, enabling precise evaluation of both regular and irregular areas by outlining the target region with either a dotted or solid line. All measurements were recorded in Excel for subsequent statistical analysis to compare and correlate findings across ages.

### **Immunohistochemical study**

The study utilized Anti-LGR5 antibody as the primary marker to detect and analyze multipotent stem cells in renal tubules, focusing on their density, distribution and expression across studied postnatal stages, using 3-micrometer paraffin sections. The procedure was conducted in accordance with the manufacturer's protocol of staining kit (ImmunoCruz LSAB rabbit staining kit [catalog no. sc-2051], Santa Cruz Biotechnology; and the primary antibody (Rabbit anti-human GPR49 kit [catalogue no. 170733], US Biological.

**Statistical analyses**

The micro-morphometric characteristics and renal histomorphometric parameters of the subjects were expressed as mean and standard error. Differences in renal tubules across age groups were analyzed using one-way ANOVA, with post-hoc pairwise comparisons conducted using the Tukey test. A significance level was set at a  $P < 0.05$ . JMP® Pro 14.3.0 was used to perform statistical calculations.

**Results**

**Histo-morphometric and Micro-developmental changes of renal tubules**

Table 1 show a consistent decrement in the mean epithelial height and luminal diameter of proximal convoluted tubule PCT from PND 1 to PND 40, with

reductions of about 2.1 2.3 folds respectively. In the same way, the distal convoluted tubule (DCT) demonstrated a decline in these parameters about 3.5 folds and 1.5 folds. PCT exhibited a smaller lumen diameter but the epithelial height was higher compared to DCT. At PND 40, the ratio of lumen-to-epithelial height of PCT's was 1:2.8, indicating a narrower lumen and taller cells, while the DCT maintained a balanced ratio of 1:1, in contrast to 2.3:1 at PND 1. Additionally, developmental changes in renal tubules were highly significant between PND 1 and 40 for all parameters ( $p < 0.0001$ ). However, several parameters showed no significant differences between specific postnatal days. For the PCT, lumen diameter and epithelial height changes were insignificant between PNDs 10-15, 15-30, and 30-40. The DCT lumen diameter showed no significant change between PNDs 15-30, while its epithelial height exhibited insignificant changes between PNDs 1-10, 10-15, and 30-40.

Table 1: Histo-morphometric parameters of renal tubules among groups of the study

Renal tubules	Groups					P-value	Pairwise Comparison
	One- day	10- days	15- days	30- days	40 -days		
PCT Lumen Diameter ( $\mu\text{m}$ )	6.69 $\pm$ 0.43	4.67 $\pm$ 0.43	4.22 $\pm$ 0.43	3.37 $\pm$ 0.43	2.85 $\pm$ 0.46	<0.0001	G1 Vs G5 ( $p < 0.0001$ ) G1 Vs G4 ( $p < 0.0001$ ) G1 Vs G3 ( $p = 0.0002$ ) G1 Vs G2 ( $p = 0.0019$ ) G2 Vs G5 ( $p = 0.0059$ ) G3 Vs G5 ( $p = 0.0347$ ) G2 Vs G4 ( $p = 0.0386$ ) G1 Vs G5 ( $p < 0.0001$ ) G1 Vs G4 ( $p < 0.0001$ ) G1 Vs G3 ( $p < 0.0001$ )
PCT Epi. Height ( $\mu\text{m}$ )	16.29 $\pm$ 0.66	10.78 $\pm$ 0.66	10.37 $\pm$ 0.66	8.25 $\pm$ 0.66	7.89 $\pm$ 0.66	<0.0001	G1 Vs G2 ( $p < 0.0001$ ) G2 Vs G5 ( $p = 0.0031$ ) G2 Vs G4 ( $p = 0.0090$ ) G3 Vs G5 ( $p = 0.0103$ ) G3 Vs G4 ( $p = 0.0272$ ) G1 Vs G5 ( $p < 0.0001$ ) G1 Vs G4 ( $p < 0.0001$ ) G1 Vs G3 ( $p < 0.0001$ ) G2 Vs G5 ( $p < 0.0001$ )
DCT Lumen Diameter ( $\mu\text{m}$ )	19.60 $\pm$ 0.78	14.29 $\pm$ 0.78	10.75 $\pm$ 0.78	9.18 $\pm$ 0.78	5.55 $\pm$ 0.78	<0.0001	G1 Vs G2 ( $p < 0.0001$ ) G3 Vs G5 ( $p < 0.0001$ ) G2 Vs G4 ( $p < 0.0001$ ) G4 Vs G5 ( $p = 0.0019$ ) G2 Vs G3 ( $p = 0.024$ ) G1 Vs G5 ( $p < 0.0001$ ) G2 Vs G5 ( $p < 0.0001$ ) G1 Vs G4 ( $p < 0.0001$ )
DCT Epi. Height ( $\mu\text{m}$ )	8.41 $\pm$ 0.28	8.08 $\pm$ 0.28	7.46 $\pm$ 0.28	6.39 $\pm$ 0.28	5.69 $\pm$ 0.28	<0.0001	G3 Vs G5 ( $p < 0.0001$ ) G2 Vs G4 ( $p = 0.0001$ ) G3 Vs G4 ( $p = 0.0110$ ) G1 Vs G3 ( $p = 0.0219$ )

PCT: Proximal Convoluted Tubules; DCT: Distal Convoluted Tubules; Epi.: Epithelium.

### General histological changes of renal tubules

Histological examination revealed a progressive growth of PCT in the inner, middle, and outer cortical zones during the postnatal periods. Microscopic investigation identified the tubules associated with glomeruli in the cortex. The PCT, the most coiled and longest segment of the renal tubules, creates from the renal corpuscles at urinary pole, occupying renal cortex with its convoluted structure. It is lined by truncated pyramidal acidophilic epithelium, with centrally located round to elliptical nuclei, while the DCT, characterized by a wider lumen and low cuboidal epithelium, lacks a brush border and shows less acidophilic characteristics than the PCT. The DCT lumen is wider than the PCT, and its wall is adjacent to afferent arteriole at vascular pole of the corpuscle (Figure 1). In rabbits aged between 30- and 40 days, the DCT displays unique morphological features at the macula densa, part of the juxtaglomerular apparatus (JGA) (Figure 2).

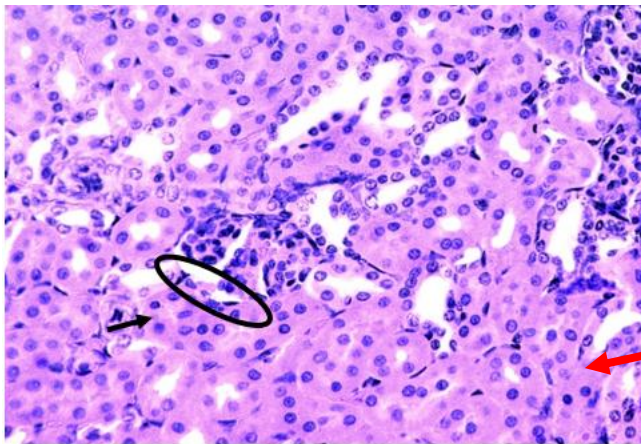


Figure 1: Histological section of renal cortex at PND 40 shows PCTs (black- arrow) which close to the glomerular urinary pole (black circle) and DCTs (red- arrow) (X400, H&E stain).

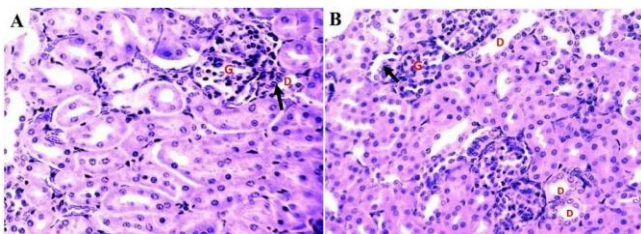


Figure 2: Histological section of renal cortex at (A) PND 30, (B) PND 40 show DCTs (D) contact with glomerular root (G), macula densa (black -arrow) (X400, H&E stain).

The PCT cells in PND-1 displayed acidophilic cytoplasm with vacuoles. Few developing PCTs were found in outer zone of cortex, whereas more of these tubules were

progressively detected toward the inner cortical zone (Figure 3A). The PCT and DCT at PND-10 showed progressive developmental changes, with slightly vacuolated and acidophilic cytoplasm of PCTs in the outer cortex. Notably, loose connective tissue with blood vessels surrounded PCTs (Figure 3B). Further nephron maturation was observed at PND-15, with increased acidophilic density in PCTs and sporadic vacuoles, while inner cortical tubules exhibited more advanced morphology than outer cortical ones (Figure 3C and D). At PND 30, the eosinophilic areas around PCT cells were distributed evenly, with occasional vacuoles and nearby blood capillaries (Figure 4A). By PND 40, the PCT showed distinct differentiation with deeply acidophilic cytoplasm, while the arrangement of blood vessels and vacuoles remained consistent with PND 30 findings (Figure 4B).

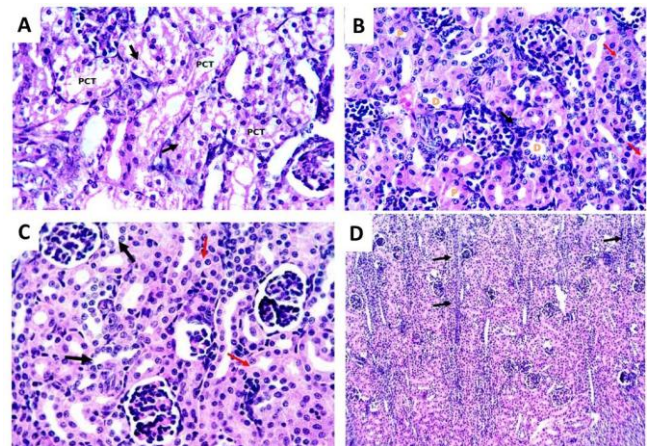


Figure 3: A- Histological section of renal cortex at PND one showing vacuolated cells with acidophilic cytoplasm of PCTs (PCT) (black-arrow) (X400, H&E stain). B- PND 10 shows less vacuolation with more acidophilic cytoplasm (red-arrow) in the PCTs (P). connective tissue was detected near PCTs (black-arrow); DCTs(D). C and D- sections of cortex at PND 15 shown that the PCTs (red-arrow) displayed a dark pink staining, while the DCTs (black arrow) displayed a lighter staining. Cortical tubules (black-arrows) (B,C: X400, D: X100 H&E stain).

The LoH, penetrate renal medulla to form descending (thin) limb across outer to inner zone of medulla, followed by an ascending (thin) limb that continue as thick limb which lined by one layer of cuboidal epithelium and ovoid nuclei. Histologic examination shows all thin segments lined by simple squamous type of epithelium with bulging nuclei that narrowing the tubule lumen. The medulla's outer region contains a straight proximal tubule segment, while the inner zone of medulla is composed of the thin as well as thick limbs of Henle's loop and collecting ducts (Figure 5).

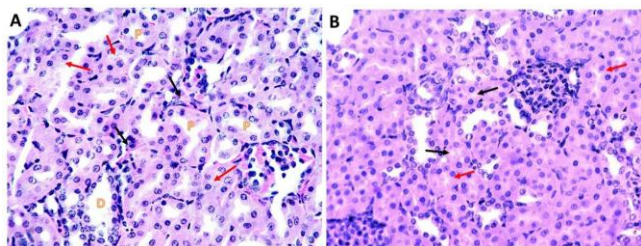


Figure 4: A-Histological section of renal cortex at PND 30 presented the homogenous distribution of acidophilic area in the cytoplasm of PCTs (P) with a small number of vacuoles (red-arrow). DCTs (D) and blood capillary (black-arrow) have been shown. B-The microphotograph of the renal cortex section at PND 40 depicts PCTs (red-arrow) characterized by its homogeneous cytoplasm. With few vacuoles (black arrow) were still present (A,B X400, H&E stain).

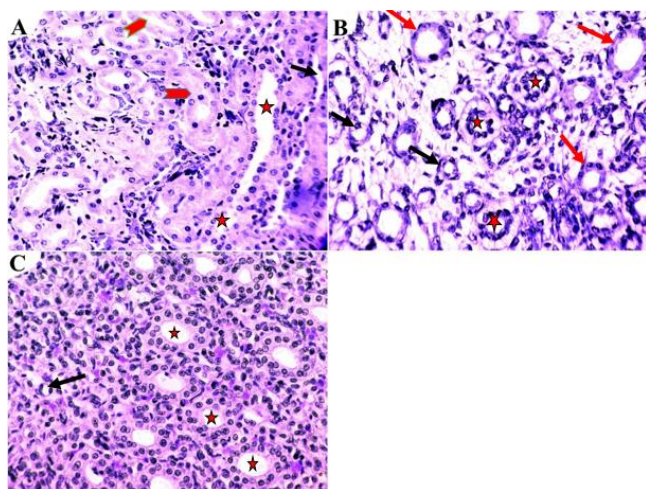


Figure 5: A-Histological section of kidney medulla at PND 40 displays (A) the outermost zone of medulla contains straight parts of proximal tubules (red chevron-arrow). It shows the CD (five-point star) and the thin segment of LoH (black arrow). B-The inner part of developed renal medulla comprises scanty connective tissue and tubules segments. Collecting ducts (five-point star) intermingled among thick and thin limbs of LoH (red, and black-arrows respectively). C-The inner zone of medulla shows thin segment of LoH (black arrow) as well as CDs (five-point star) (X400 H&E stain).

At PND 1, outer medulla appeared disorganized, comprising compact primitive tubule bundles with large lumens. this region contains vacuolated CDs, lined with tall cuboidal cells, immersed in loose interstitial and mesenchymal tissue. The inner medulla, however, contained dense clusters of collecting ducts and LoH segments with negligible connective tissue (Figure 6A and 6B). By PND 10,

the outer medulla exhibited increased organization, enhanced tubule prominence, and elongation, with reduced interstitial tissue and a discernible increase in LoH numbers. Straight segment of proximal tubules and CDs turn out to be clearer, while the inner zone of medulla remained primarily composed of LoH and CDs with limited stroma (Figure 6C and 6D).

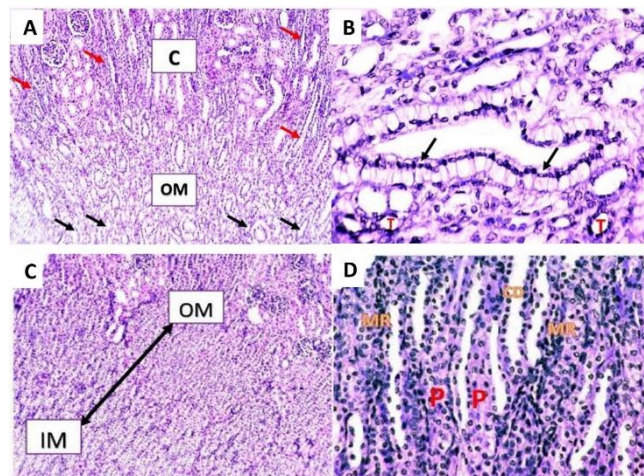


Figure 6: A- The microphotograph of kidney cortex (C) and the outermost medulla (OM) at PND one. Show disorganized outer piece of the primitive medulla which constitute of primitive tubules (black-arrow), medullary rays (red-arrow). B- High magnification of inner zone of medulla of figure-A show some vacuolated cells in the branched CD (black arrows); thin-limb of LoH (T). C- The microphotographs of the kidney sections at PND 10 show (A) the well-defined demarcation between the outer medulla (OM) and inner medulla (IM) (double-headed arrow). D- Show straight segments of proximal tubules (P) and CDs (CD) can be observed with clear medullary ray (MR) (A,C X100, B & D: X400 H&E stain).

At PND-15, tubular differentiation between the outer and inner zones of medulla became more noticeable by an acidophilic zone. Tubules, medullary rays and CDs extended toward the cortical and subcortical zones and connective tissue observed among them. The outer medulla contained thick and thin segments of the LoH and CD, with cuboidal cells displaying variable staining and vacuoles. The thick segments of the LoH were immature and difficult to distinguish from CDs. The inner zone of medulla in the same way contained collecting ducts a thick and thin LoH (Figure 7).

At PND-30, the medullary thickness increased significantly, giving the kidneys a mature morphology with a distinct separation between inner and outer zones of medulla. The outer area of medulla exhibited defined inner and outer bands, along with prominent maturation in

collecting ducts as well as segments of LoH. By day 40, the kidneys appeared morphologically mature, with denser medulla containing more tubules collecting ducts and elongated loops. The LoH's thin and thick portions were well-differentiated, surrounded by vasa recta capillaries. The thick descending LoH resembled the PCT in the cortex, while the thick ascending LoH resembled the DCT (Figure 8). CDs were divided into cortical, lined by simple cuboidal epithelium, and medullary types, lined by high cuboidal epithelium.

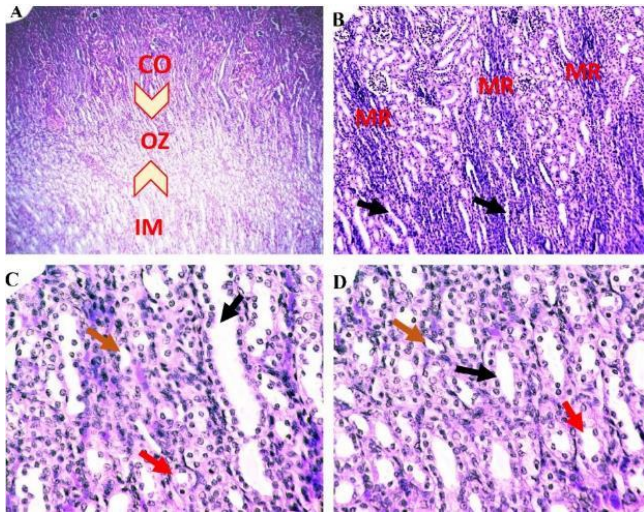


Figure 7: The microphotographs of kidney sections at PND 15 show: A- the distinction between the inner and outer medulla was more obvious. The outer zone (OZ) of the medulla can be seen (area between two chevron arrows), separating the cortex (CO) from inner medulla (IM). B- The medullary ray (MR), and collecting tubules (black arrow) are present in the subcortical and cortical zones. C- The outer medulla contained thick segment (red arrow), thin segment (brown arrow), and CD (black arrow). D- The inner medulla showed thin segment (brown arrow), thick segment (red arrow) of LoH, and CD (black arrow) (A: X40, B: X100, C&D: X400, H&E).

**Histochemical findings of renal tubules**

In all age groups, combined PAS and AB staining produced a moderate positive reaction in the PCTs' brush border and basement membrane, and a strong AB response on the luminal surface of some DCTs (pH 2.5) (Figure 9). The combined PAS-AB (pH 2.5) staining revealed acidic mucopolysaccharides in in all studied groups, with a significantly stronger response to AB staining observed with age advancement (Figure 10).

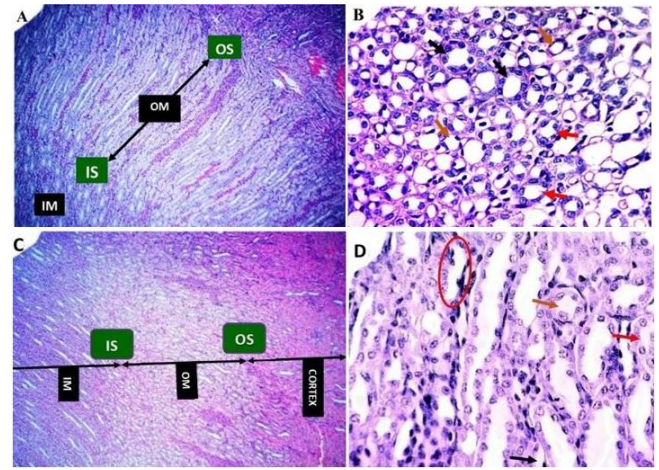


Figure 8: The microphotographs of the kidney sections at PND 30 show A- the obvious distinction between outer medulla (OM) and inner medulla (IM). The inner strip (IS) and outer strip (OS) of outer zone of medulla could be easily distinguished. B- Obviously the thick segment (red-arrows) and thin segment (brown-arrows) of LoH in the medulla were more differentiated, the CDs (black arrows) can be observed. C, D- At PND 40, kidney microphotographs show increased medulla thickness, distinguishing the inner (IM) and outer medulla (OM), with clear separation of the outer medulla's inner (IS) and outer strips (OS). The medulla contains thick (brown arrow) and thin (black arrow) LoH segments, vasa recta (red circled area), and straight PCT segments (red arrow) (A,C: 4X0, B,D: X400, H&E).

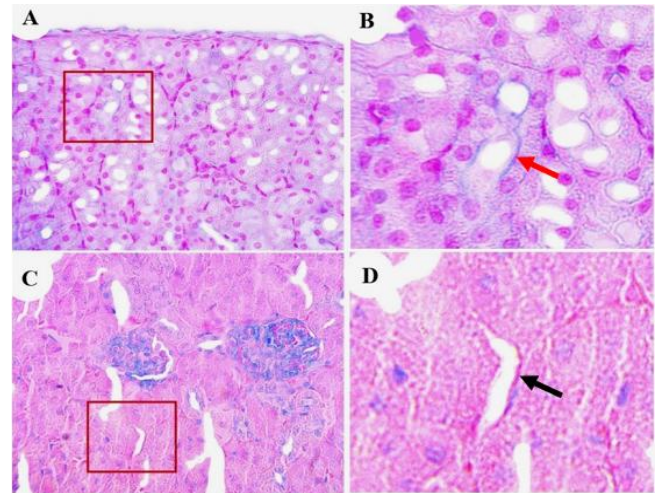


Figure 9: The microphotograph sections of the renal cortex at (A) PND 15, and (B) its magnification, show strong positive reaction (blue color) toward AB to the luminal surface of some DCTs (red arrow). At (C) PND 30, and (D) its magnification, the brush border and basement membrane of some proximal tubules show moderate reaction (magenta-color) with the PAS (black arrow) (X400, PAS-AB).

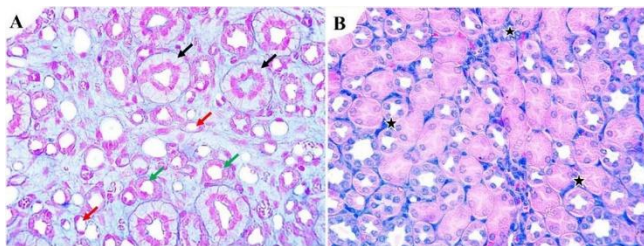


Figure 10: Histological sections of renal medulla staining with the combined PAS-AB show that at (A) PND one, the collecting ducts (black-arrow), thick segment (green-arrow) and thin segments (red-arrow) of the LoH moderately respond (light-blue color) to AB stain, and at (B) PND 40, strongly respond (dark-blue) (five-point star) to AB stain (X400, PAS-AB).

### Immunohistochemical characteristics of renal tubules

The PCT and DCT showed negative reaction against Lgr5 in all studied groups (no staining, score 0). Positive cells were seen in the interstitial tissues among LoH (Figure 11) showed Lgr5 positive cells; The immunostaining positive cells in the interstitial tissue surrounding LoH revealed moderate immunopositive reaction for Lgr5 diffusely seen at PND one. Whereas, there was a weak-to-moderate immunostaining in the interstitial tissue diffusely found at PND 10 compared to the rabbits in the PND 15 that revealed a weak positive cell staining focally. Moreover, the expression of Lgr5 in renal interstitial tissue were suppressed at PNDs 30 and 40.

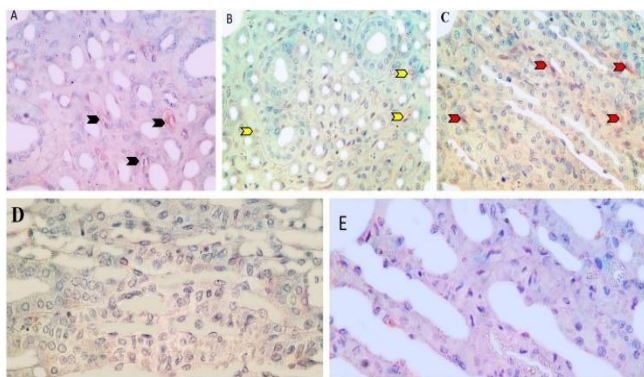


Figure 11: Immunohistochemical staining of Lgr5 cytoplasmic immunostaining of the LoH of renal tissue sections of the 40-day aged rabbit. (A) moderate expression of Lgr5 (score 9) in the interstitial tissues among LoH (black chevron-arrow), (B) weak to moderate expression against Lgr5 (score 6) in the interstitial tissues among LoH (yellow chevron-arrow), (C) Lgr5 weakly reacted (score 2) among the interstitial tissues surrounding the segments of the LoH, (D and E) no reaction (score 0) of Lgr5 have been illustrated in the interstitial tissues among LoH (X400; IHC, Anti-Lgr5).

### Discussion

Postnatal renal development differs significantly from adult kidney function. Animal models, particularly rabbits, are key for understanding tissue maturation and variability (20). This study aims to identify critical developmental stages in rabbit kidney tubules, providing a reference for assessing the impact of chemicals on kidney development and aiding future research interpretations. The findings the current study confirm that renal development, including tubulogenesis, progresses postnatally and reaches completion by PND 40 (21). Although our findings primarily focus on postnatal renal tubular development, we believe they align with the embryonic and fetal kidney study by Seriola (22). This study reported that nephron formation, induction, and organization begin when the urinary buds invade the nephrogenic mesenchyme. At this stage, a subset of cells condenses and undergoes direct proliferation, forming pretubular clusters. These clusters subsequently differentiate into secretory nephron epithelium, which eventually segments into distinct tubule structures. Parker and Picut (23) reported that rat kidneys remain histologically immature until PND 30, with nephrogenesis completing after birth, similar to rabbits (16). This postnatal kidney development makes these animals ideal for studying fetal and neonatal renal function. In contrast, species like spiny mice, humans, and sheep complete nephrogenesis before birth (24-26), while postnatal renal medulla development continues in humans (27). Other species, such as pigs and dogs, also show delayed nephrogenesis, finishing well after birth (28,29).

This study observed a progressive decrease in both the average tubular lumen diameter and epithelial height in PCTs and DCTs from birth to PND 40. A reduction in cell number within these tubules was also noted, indicating a significant overall reduction in renal tubule size as the rabbits matured. These findings are consistent with Niborski *et al.* (30), who reported extensive tubular elongation due to cell proliferation during the early postnatal period in mice, followed by a decline in proliferation post-weaning. Additionally, PCTs exhibited a smaller lumen diameter but greater epithelial height compared to DCTs, which aligns with previous studies showing variations in microvilli distribution in PCTs (31,32). This observation is similar to Friis (33), who reported decreased cell height in pig proximal tubules with varying microvilli length. While Şimşek *et al.* (34) noted DCT and PCT continue in development until postnatal day 20, the present study found that development of renal tubule in rabbits extended till day 40.

Current study, consistent with previous research (35-37), found that renal tubules newly born kits showed completed histogenesis throughout the embryonic life, whereas renal corpuscle development continued until postnatal day 15 (16, 23). Microscopic and morphometric analyses in the current study revealed the maturation of

proximal tubules in the inner, middle, and outer cortex regions of the developing rabbit kidney. The study also observed congestion in glomerular capillaries and surrounding blood vessels, contrasting with Alyahya (38), who reported minimal vascular presence in domestic rabbits. Additionally, this research noted that the PCTs had a narrow lumen lined with cuboidal epithelium and centrally located nuclei, differing from Al-Sharoot (39) findings in pigs, where PCTs had wider lumens. Such differences may be attributed to species-specific adaptations, as indicated by El-Salkh *et al* (40). Furthermore, our findings differ from Ajayi *et al* (41) who observed columnar epithelium lining the PCTs in grasscutters, an African rodent. In contrast, our results align with those of Al-Salami (42) in camels, Hussin (43) in dogs, and Faidh Baragoth *et al* (29) in rats, which reported small PCT lumens associated with reduced urine dilution. These results also contrast with Yousif and Rabee (44) who found that guinea pig DCTs were shorter with narrower lumens than PCTs. Additionally, in mice, the DCT resembled the PCT, while in humans, it was lined with less eosinophilic cuboidal epithelium (45).

This study identified the presence of PAS-positive granules in the PCT of rabbit kidneys during various postnatal stages, indicating moderate to strong reactions, while the DCT, LoH, and collecting tubules showed weaker PAS-AB staining. This suggests differential carbohydrate content across tubular segments. Consistent with other species, such as rats, rabbits, and male guinea pig (44,45), the PCTs exhibited substantial glycogen and glycoprotein accumulation, reflecting high metabolic activity. The study's findings also align with observations in herbivores like cows and goats, where the PCTs displayed intense PAS staining due to elevated glycogen content (46).

Previous finding indicated strong Lgr5 expression in one-day-old rabbits, particularly in podocytes and mesangial cells of newly formed glomeruli, which decreased with age and was suppressed by PND 30 (16). This suggests Lgr5 as a marker for glomerular and nephron development, with its expression confined to immature developing nephrons. Therefore, Lgr5 could be valuable for identifying and isolating epithelial progenitor cells in newborn rabbit kidneys, with potential applications in regenerative medicine for chronic renal diseases and congenital disorders in humans. Intriguingly, Barker *et al* (13) observed Lgr5 expression during early kidney development in mouse models, coinciding with key nephrogenesis phases. Habib and Alhaaik (23) indicated that Lgr5<sup>+</sup>ve cells in nascent nephrons may generate other Lgr5<sup>-</sup>ve cells during early postnatal nephrogenesis. In adult kidneys, Lgr5 expression is minimal under normal conditions but may be reactivated following injury (38,39). Although our study focused on postnatal renal tubular development, previous research showing the absence of Lgr5 in adult human and mouse kidneys (4,40). These studies suggest that Lgr5 may be

temporarily reactivated in adult kidneys following injury. Finally, On PND 1, we observed moderate Lgr5 expression in the connective tissue within the renal medulla, papillae, pelvis, and interstitial tissues surrounding segments of the LoH. By PNDs 10 and 15, Lgr5 expression declined to mild levels and was undetectable in kits aged 30 and 40 days. These findings align with previous studies (41,42) that reported a lack of antibodies specific to the thin ascending limb of the LoH in animal models. This IHC analysis also revealed no Lgr5 expression in the uriniferous tubules. However, there was moderate Lgr5 expression in blood vessels and interstitial tissues of the renal cortex on PND 1, which diminished by PNDs 10 and 15. Additionally, the vascular pole of the glomeruli exhibited moderate Lgr5 expression on PND 1, decreasing significantly by PNDs 10 and 15, with no detectable expression at the urinary pole.

The expression of Lgr5 as a marker for stem/progenitor cells in the kidney has significant implications for renal repair and regeneration. Previous studies have demonstrated that Lgr5<sup>+</sup>ve cells contribute to nephron formation during kidney development (47). These findings suggest that Lgr5-expressing cells may serve as a potential target for regenerative therapies, particularly in conditions where kidney injury leads to irreversible nephron loss. In cases of renal injury, the ability of intrinsic epithelial cells to contribute to kidney repair is well-documented (48). While the adult kidney has limited regenerative capacity, studies suggest that certain populations of epithelial progenitor cells, including Lgr5<sup>+</sup>ve stem-like cells, could play a role in repairing damaged tubular structures. Understanding the behavior of Lgr5-expressing cells in postnatal development may provide insights into their therapeutic potential for kidney injuries in veterinary medicine, particularly in species susceptible to acute or chronic renal damage. Furthermore, studies on early nephron patterning indicate that proliferation within renal vesicles contributes to nephron segmentation and functional differentiation (49). This underscores the importance of Lgr5<sup>+</sup>ve progenitors in the organization of renal structures, which may be critical for optimizing strategies aimed at tissue engineering and regenerative therapies for kidney diseases in veterinary and translational medicine.

Building on previous research, our latest publication (23), and the finding of the current study, we believe that expanding research on Lgr5-mediated renal regeneration could provide a foundation for novel therapeutic interventions in veterinary and human nephrology, focusing on enhancing natural repair mechanisms or utilizing Lgr5<sup>+</sup>ve cells in regenerative approaches.

**Strength and Limitations:** Unfortunately, this study did not include all PNDs from day one to day 40, which would have offered a more detailed understanding of the structural changes observed throughout development. Furthermore, the investigation did not assess additional potential renal stem

cell markers, limiting the scope of insights into renal development.

## Conclusions

This study offers in-depth study of postnatal renal tubule development in rabbits, focusing on histological, histochemical, morphometric, and immunohistochemical attributes. Results indicate a constant decrement in epithelial height and lumen diameter of both PCT and DCT from birth to PND 40, reflecting substantial structural modifications during this period. The lack of *Lgr5* expression in renal tubules, coupled with its variable presence in interstitial tissues around the LoH, suggests its involvement in early nephron development. These findings enhance the understanding of renal organogenesis and may inform regenerative therapeutic strategies for kidney disorders.

## Acknowledgment

The authors express their sincere thankfulness for the support and facilities provided by Mosul University/College of Veterinary Medicine.

## Conflict of interests

The authors declared they have no competing interests.

## References

1. El-Bestawy EM, Hegab AS, Abdel Hamid RA, Sewelam AS. Postnatal developmental changes of the kidneys of the albino rat. *Egypt J Hosp Med.* 2017;69(6):2711-21. DOI: [10.12816/0042254](https://doi.org/10.12816/0042254)
2. Little MH, McMahon AP. Mammalian kidney development: principles, progress, and projections. *Cold Spring Harb Perspect Biol.* 2012;4(5):a008300. DOI: [10.1101/cshperspect.a008300](https://doi.org/10.1101/cshperspect.a008300)
3. Little M, Georgas K, Pennisi D, Wilkinson L. Kidney development: two tales of tubulogenesis. *Curr Top Dev Biol.* 2010;90:193-229. DOI: [10.1016/s0070-2153\(10\)90005-7](https://doi.org/10.1016/s0070-2153(10)90005-7)
4. Schwartz GJ, Olson J, Kittelberger AM, Matsumoto T, Waheed A, Sly WS. Postnatal development of carbonic anhydrase IV expression in rabbit kidney. *Am J Physiol Renal Physiol.* 1999;276(4):F510-20. DOI: [10.1152/ajprenal.1999.276.4.f510](https://doi.org/10.1152/ajprenal.1999.276.4.f510)
5. Fayez E, Sayed-Ahmed A, Abo-Ghanema II, Elnasharty MA. Morphogenesis of rabbit kidney pre- and postnatal. *Alexandria J Vet Sci.* 2014. DOI: [10.5455/ajvs.154807](https://doi.org/10.5455/ajvs.154807)
6. Quaggin SE, Kreidberg JA. Development of the renal glomerulus: good neighbors and good fences. *Development.* 2008;135(4):609-20. DOI: [10.1242/dev.001081](https://doi.org/10.1242/dev.001081)
7. Woodhall PB, Tisher CC, Simonton CA, Robinson RR. Relationship between para-aminohippurate secretion and cellular morphology in rabbit proximal tubules. *J Clin Invest.* 1978;61(5):1320-9. DOI: [10.1172/jci109049](https://doi.org/10.1172/jci109049)
8. Imai M, Kaissling B, Maunsbach A, Moffat D, Natchin Y. A standard nomenclature for structures of the kidney. *Kidney Int.* 1988;33:1-7. DOI: [10.1038/ki.1988.1](https://doi.org/10.1038/ki.1988.1)
9. Kaissling B, Kriz W. Structural analysis of the rabbit kidney. Germany: Springer; 1979. [\[available at\]](#)
10. Bankir L, De Rouffignac C. Urinary concentrating ability: insights from comparative anatomy. *Am J Physiol Regul Integr Comp Physiol.* 1985;249(6):R643-66. DOI: [10.1152/ajpregu.1985.249.6.r643](https://doi.org/10.1152/ajpregu.1985.249.6.r643)
11. Gullans SR, Blumenfeld JD, Balschi JA, Kaleta M, Heilig CW, Cohen DM. Accumulation of major organic osmolytes in rat renal inner medulla in dehydration. *Am J Physiol Renal Physiol.* 1988;255(4):F626-34. DOI: [10.1152/ajprenal.1988.255.4.f626](https://doi.org/10.1152/ajprenal.1988.255.4.f626)
12. Ridderstrale Y, Kashgarian M, Koeppen B, Ardito T, Laurent TC, Carone FA. Morphological heterogeneity of the rabbit collecting duct. *Kidney Int.* 1988;34(5):655-70. DOI: [10.1038/ki.1988.230](https://doi.org/10.1038/ki.1988.230)
13. Barker N, Rookmaaker MB, Kujala P, Ng A, Leushacke M, Snippet HJ, van de Wetering M, Tan S, Van Es JH, Huch M, Poulsom R, Verhaar MC, Peters PJ, Clevers H. *Lgr5<sup>+</sup>* stem/progenitor cells contribute to nephron formation during kidney development. *Cell Rep.* 2012;2(3):540-52. DOI: [10.1016/j.celrep.2012.08.018](https://doi.org/10.1016/j.celrep.2012.08.018)
14. Pulkkinen K, Murugan S, Vainio S. Wnt signaling in kidney development and disease. *Organogenesis.* 2008;4(2):55-9. DOI: [10.1016/bs.pmbts.2017.11.019](https://doi.org/10.1016/bs.pmbts.2017.11.019)
15. Schunk SJ, Floege J, Fliser D, Speer T. WNT- $\beta$ -catenin signalling: a versatile player in kidney injury and repair. *Nat Rev Nephrol.* 2021;17(3):172-84. DOI: [10.1038/s41581-020-00343-w](https://doi.org/10.1038/s41581-020-00343-w)
16. Habib RS, Alhaaik AG. Age-related glomerular histogenesis in inbred indigenous rabbit (*Oryctolagus cuniculus*): a morphological, morphometrical, and immunohistochemical study with emphasis on *Lgr5*-positive cells. *Acta Histochem.* 2023;125(1):151994. DOI: [10.1016/j.acthis.2022.151994](https://doi.org/10.1016/j.acthis.2022.151994)
17. Baneux P, Garner D, McIntyre H, Holshuh H. Euthanasia of rabbits by intravenous administration of ketamine. *J Am Vet Med Assoc.* 1986;189(9):1038-9. [\[available at\]](#)
18. McDowell EM, Trump BF. Histologic fixatives suitable for diagnostic light and electron microscopy. *Arch Pathol Lab Med.* 1976;100(8):405-14. [\[available at\]](#)
19. Suvarna KS, Layton C, Bancroft JD. Bancroft's theory and practice of histological techniques. London, UK: Elsevier Health Sciences; 2018. [\[available at\]](#)
20. Mapara M, Thomas BS, Bhat K. Rabbit as an animal model for experimental research. *Dent Res J.* 2012;9(1):111-8. DOI: [10.4103/1735-3327.92960](https://doi.org/10.4103/1735-3327.92960)
21. Saxén L. Organogenesis of the kidney. Cambridge, UK: Cambridge University Press; 1987. DOI: [10.1017/CBO9780511565083](https://doi.org/10.1017/CBO9780511565083)
22. Sariola H. Nephron induction revisited: from caps to condensates. *Curr Opin Nephrol Hypertens.* 2002;11(1):17-21. DOI: [10.1097/00041552-200201000-00003](https://doi.org/10.1097/00041552-200201000-00003)
23. Parker GA, Picut CA. Atlas of histology of the juvenile rat. Cambridge, MA: Academic Press; 2016. [\[available at\]](#)
24. Dickinson H, Walker DW, Cullen-McEwen L, Wintour EM, Moritz K. The spiny mouse (*Acomys cahirinus*) completes nephrogenesis before birth. *Am J Physiol Renal Physiol.* 2005;289(2):F273-9. DOI: [10.1152/ajprenal.00400.2004](https://doi.org/10.1152/ajprenal.00400.2004)
25. Guron G, Friberg P. An intact renin-angiotensin system is a prerequisite for normal renal development. *J Hypertens.* 2000;18(2):123-37. DOI: [10.1097/00004872-200018020-00001](https://doi.org/10.1097/00004872-200018020-00001)
26. Joana P, Justina P, Lígia B, Paula R, Isabel P. Histochemical and immunohistochemical study of peripolar cells in sheep. *J Histol.* 2013;2013:237630. DOI: [10.1155/2013/237630](https://doi.org/10.1155/2013/237630)
27. Li J, Guandalini M, McInnes H, Kandasamy Y, Trnka P, Moritz K. The impact of prematurity on postnatal growth of different renal compartments. *Nephrology.* 2020;25(2):116-24. DOI: [10.1111/nep.13623](https://doi.org/10.1111/nep.13623)
28. Bragulla H. The development of the metanephric kidney in the pig. *Anat Histol Embryol.* 2005;34:7-7. DOI: [10.1111/j.1439-0264.2005.00669.15.x](https://doi.org/10.1111/j.1439-0264.2005.00669.15.x)
29. Faidh Baragoth A, Ghazi HAA-M, AbdZaid K. Histological study of the nephrons of the kidney in dogs (*Canis familiaris*) in middle Iraq. *Kufa J Vet Med Sci.* 2014;5(1). [\[available at\]](#)
30. Niborski LL, Guichard C, Hanssens I, Deleuze JF, Martinovic J, Clement-Ziza M. Hnf1b haploinsufficiency differentially affects developmental target genes in a new renal cysts and diabetes mouse model. *Dis Model Mech.* 2021;14(5):dmm047498. DOI: [10.1242/dmm.047498](https://doi.org/10.1242/dmm.047498)

31. El-Gammal A, Ibrahim OY, Shaban SF, Dessouky AA. Postnatal development of the albino rat renal cortex (histological study). Egypt J Histol. 2010;33(4):745-56. [\[available at\]](#)
32. Gaffiero P, Bergeron M, Thiery G. Morphological study of cell organelles during development II—the mitochondria of the renal and intestinal epithelium. Biol Cell. 1984;49(2):163-8. DOI: [10.1111/j.1768-322x.1984.tb00234.x](#)
33. Friis C. Postnatal development of the pig kidney: ultrastructure of the glomerulus and the proximal tubule. J Anat. 1980;130(Pt 3):513-22. [\[available at\]](#)
34. Şimşek N, Altunkaynak BZ, Ünal D, Can S, Malkoç I, Ünal B. A stereological and electron microscopic study of the development of the nephron in prenatal and postnatal rats. Eurasian J Med. 2009;41(2):84-91. [\[available at\]](#)
35. Okada T, Morikawa Y. Development of the proximal tubule of the fetal rat kidney: morphometry and ultrastructural findings. Ann Anat. 1993;175(1):89-94. DOI: [10.1016/s0940-9602\(11\)80248-7](#)
36. Yağın E, Ünal I, Kirlioglu E, Atilla P, Müftüoğlu S, Karnak İ. Investigation of obstructive uropathy for histopathologic changes and apoptosis in urinary system of Adriamycin-exposed rat fetuses. In: 15th International Congress of Histochemistry and Cytochemistry. Turkey; 2017. DOI: [10.5505/2017ichc.OP-19](#)
37. Yuluğ E, Ünal I, Kirlioglu E, Atilla P, Müftüoğlu S, Karnak İ. Biochemical and morphological evaluation of the effects of propolis on cisplatin-induced kidney damage in rats. Biotech Histochem. 2019;94(3):204-13. DOI: [10.1080/10520295.2018.1543895](#)
38. Alyahya ARA. Comparative histological studies of the kidney, liver and testes of the adult male domestic and wild rabbits (*Oryctolagus cuniculus*) in Saudi Arabia. J Am Sci. 2015;11(12). DOI: [10.7537/marsjas111215.35](#)
39. Al-Sharoot HA. Morphological and histological study of the kidney in guinea pig. Int J Recent Sci Res. 2014;5(11):1973-6. [\[available at\]](#)
40. El-Salkh BA, Khidr HA, Zaki ZT, Basuony MI. Anatomical, histological and histochemical studies on some organs of true desert rodents in the Egyptian habitats. Egypt J Hosp Med. 2008;33(1):578-606. [\[available at\]](#)
41. Ajayi IE, Ojo SA, Ayo JO, Ibe CS. Histomorphometric studies of the urinary tubules of the African grasscutter (*Thryonomys swinderianus*). J Vet Anat. 2010;3(1):17-23. DOI: [10.21608/jva.2010.44903](#)
42. Al-Salami N. Microscopic study of some parts of urinary system in one-humped dromedary camel, especially the kidney [master's thesis]. Iraq: College of Veterinary Medicine, University of Baghdad; 1992. 19-30 p. [\[available at\]](#)
43. Hussin A. Seasonal histological changes in kidney of one-humped camel (*Camelus dromedarius*) in middle Iraq. [master's thesis]. Iraq: College of Veterinary Medicine, University of Baghdad; 2003. 29-32 p. [\[available at\]](#)
44. Delaney MA, Kowalewska J, Treuting PM. Urinary system. In: Treuting PM, Dintzis SM, Montine KS, editors. Comparative Anatomy and Histology. USA: Elsevier; 2018. 275-301 p. DOI: [10.1016/B978-0-12-381361-9.00016-0](#)
45. Al-Samawy ER. Morphological and histological study of the kidneys of the albino rats. Al-Anbar J Vet Sci. 2012;5(1):115-9. [\[available at\]](#)
46. Oghoverere AB, Igho OE. Comparative histochemical study of the kidney of six mammalian species. J Med Sci. 2019;51(1):11-23. DOI: [10.19106/JMedSci/005101201902](#)
47. Benigni A, Morigi M, Remuzzi G. Kidney regeneration. Lancet. 2010;375(9722):1310-7. DOI: [10.1016/S0140-6736\(10\)60237-1](#)
48. Humphreys BD, Valerius MT, Kobayashi A, Mugford JW, Soeung S, Duffield JS, McMahon AP, Bonventre JV. Intrinsic epithelial cells repair the kidney after injury. Cell Stem Cell. 2008;2(3):284-91. DOI: [10.1016/j.stem.2008.01.014](#)
49. Georgas K, Rumballe B, Valerius MT, Chiu HS, Thiagarajan RD, Lesieur E, Aronow BJ, Brunskill EW, Combes AN, Tang D, Taylor D, Grimmond SM, Potter SS, McMahon AP, Little MH. Analysis of early nephron patterning reveals a role for distal RV proliferation in fusion to the ureteric tip via a cap mesenchyme-derived connecting segment. Dev Biol. 2009;332(2):273-86. DOI: [10.1016/j.ydbio.2009.05.578](#)

## دراسة تطور النبيبات الكلوية بعد الولادة في الأرنب المحلي: دراسة نسيجية وكيميائية نسيجية مناعية

رونك صابر حبيب<sup>١</sup> و عمار غانم الحانك<sup>٢</sup>

<sup>١</sup> فرع علم تناسل الحيوان، التشريح والفلسفة، كلية الطب البيطري، جامعة دهوك، دهوك، <sup>٢</sup> فرع التشريح، كلية الطب البيطري، جامعة الموصل، الموصل، العراق

### الخلاصة

بينت هذه الدراسة تطور النبيبات الكلوية بعد الولادة في الأرنب المحلي، وفحص الخصائص النسيجية والكيميائية النسيجية المناعية والشكلية القياسية من الولادة إلى عمر ٤٠ يوماً. تم تقسيم خمسين أرنباً إلى خمس مجموعات عمرية بناءً على عمر ما بعد الولادة ١ و ١٠ و ٣٠ و ٤٠ يوماً. ثبتت الكلى وتمت معالجتها وتقطيعها للصبغ بملون الهيماتوكسيلين والايوسين وملون حامض شيف النوري-الاليثيان الزرقاء، تلا ذلك الفحص المجهرى. استخدمت الكيمياء النسيجية المناعية لأجسام مضادة لمستقبلات البروتين ج المقترنة بالبروتين الغني باليوسين الخامس للكشف عن الخلايا الجذعية. تم إجراء القياسات الشكلية يدوياً باستخدام كاميرا رقمية نوع أوماكس. أشارت النتائج إلى أنه بالرغم من اكتمال تنسج النبيبات الكلوية في الأرانب التي يبلغ عمرها يوماً واحداً خلال الحياة الجنينية، إلا أنها استمرت في التطور حتى اليوم الأربعين بعد الولادة. لوحظ انخفاض تدريجي في ارتفاع الظهارة وقطر التجويف في النبيبات الملنوية الداني والقاصية، حيث أظهرت النبيبات الملنوية الدانية انخفاضاً بمقدار ٢,٣ ضعفاً و ٢,١ ضعفاً على التوالي، وأظهر النبيبات الملنوية القاصية انخفاضاً بمقدار ٣,٥ ضعفاً في قطر التجويف وانخفاضاً بمقدار ١,٥ ضعفاً في ارتفاع الظهارة. ومن المثير للاهتمام، لم يلاحظ التعبير عن مستقبلات البروتين ج المقترنة بالبروتين الغني باليوسين الخامس، في النبيبات الملنوية الدانية والقاصية ولوحظ في الأنسجة الخلالية المحيطة بعروة هنلي، حيث كان تعبير معتدل في عمر يوم واحد، ثم انخفض تدريجياً بعد ذلك. توفر هذه النتائج رؤى قيمة حول نضوج النبيبات الكلوية وتضع الأساس لأبحاث مستقبلية في نمو الكلى والطب التجديدي.